Journal Website: https://www.icjn.net/jswvcm ISSN: 3106-5139 | EISSN: 3106-5147

Journal of Solid Waste Valorization and Chemical Management (JSWVCM)

ICJN Press Volume. 01 | Issue. 02 | Aug. 2026 DOI: 10.66729/jswvcm202607008

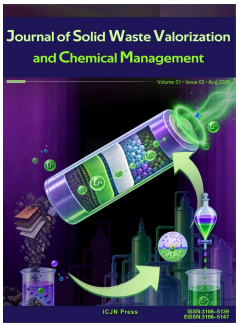

ARTICLE

Synergistic Pathways for Pollution and Carbon Reduction in End-of-Life Nickel Cobalt Manganese Oxide Battery Recycling Processes

Xi Tian[1,2,3], Ziying Zhang[3], Wei Liu[3,4,*], Xinxue Lai[5], Tongzhu Zhang[5], Hu Liu[6], Yaobin Liu[1,3,7]

1 Research Center for Central China Economic and Social Development, Nanchang University, Nanchang Jiangxi 330031, China.
2 Engineering Research Center of Watershed Carbon Neutralization, Ministry of Education, Nanchang University, Nanchang Jiangxi 330031, China.
3 School of Economics and Management, Nanchang University, Nanchang Jiangxi 330031, China.
4 School of Environment, Tsinghua University, Beijing 100084, China.
5 China Automotive Technology and Research Center Co., Ltd., Tianjin 300300, China.
6 School of Physics and Materials Science, Nanchang University, Nanchang Jiangxi 330031, China.
7 College of Applied Economics, Jiangxi University of Finance and Economics, Nanchang Jiangxi 330013, China.

*Corresponding Author: Wei Liu, Email: xueshu2019lw@163.com

Abstract

Synergistic pollution and carbon reduction in end-of-life (EOL) lithium-ion battery recycling are essential for the green and low-carbon transition of the battery recycling industry. However, systematic comparisons of different recycling processes from a synergy perspective remain limited. This study applies life cycle assessment to compare four representative recycling routes for EOL lithium nickel cobalt manganese oxide (NCM) batteries in China: pyrometallurgical recycling, hydrometallurgical recycling, pyro-hydrometallurgical recycling, and direct recycling. Environmental performance is evaluated across 18 impact categories using the ReCiPe 2016 midpoint method, and contribution hotspot analysis, sensitivity analysis, scenario analysis, and a synergy index (SI) are integrated to identify key burden sources and potential for synergistic optimization. The results show that direct recycling performs best under the baseline scenario, with the lowest burdens in 12 of the 18 impact categories and the lowest global warming potential (GWP) of 1.35 kg CO_2-eq EOL NCM battery. Key influencing parameters differ markedly among processes. Scenario analysis shows that technological progress yields the most stable synergistic benefits; under this scenario, direct recycling achieves nearly synchronized reductions in pollution and carbon, with pollution-related SI values ranging from 0.96 to 0.99. In contrast, energy structure transition substantially reduces GWP, with a 64.43% reduction for pyro-hydrometallurgical recycling, but may induce non-carbon environmental burden shifting, particularly in terrestrial ecotoxicity and ozone depletion. The combined scenario achieves high absolute reduction potential, but its synergy depends on whether pollution-related impacts decrease synchronously with GWP. Process-specific strategies that integrate source-oriented technological improvements, electricity decarbonization, and key input reduction are essential to achieve robust pollution-carbon synergies in EOL NCM battery recycling.

Keywords

Ternary lithium battery; Pollution and carbon reduction; Synergy; Recycling; Life cycle assessment

Citation: Xi Tian, Ziying Zhang, Wei Liu, *et al*. Synergistic Pathways for Pollution and Carbon Reduction in End-of-Life Nickel Cobalt Manganese Oxide Battery Recycling Processes. *Journal of Solid Waste Valorization and Chemical Management*. 2026, 01 (2):1-14. doi: 10.66729/jswvcm202607008.

Copyright:© 2026 The Author(s). Published by ICJN Press.
This is an open access article under the https://creativecommons.org/licenses/by/4.0/
Received 9 July 2026; Revised 24 July 2026; Accepted 18 August 2026; Available online 27 August 2026.

Graphical Abstract

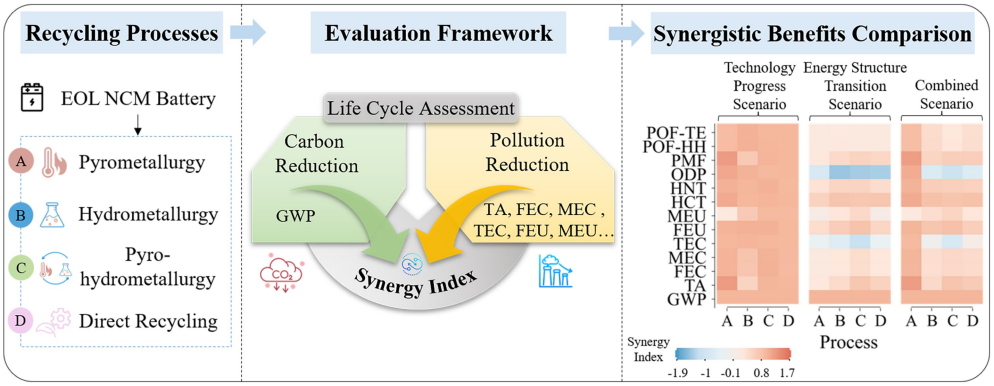

Copyright: The authors.

Highlights

- Four EOL NCM recycling routes were compared across 18 impact categories.
- Direct recycling had the lowest GWP but showed resource-toxicity trade-offs.
- Technological progress yielded steadier synergies than electricity decarbonization.

1. Introduction

Climate change mitigation and pollution control are increasingly recognized as interconnected challenges in sustainable development[1]. On September 22, 2020, China announced the "dual-carbon" goals of peaking carbon emissions before 2030 and achieving carbon neutrality before 2060[2]. In March 2026, the Outline of the Fifteenth Five-Year Plan for National Economic and Social Development of the People's Republic of China further emphasized the coordinated promotion of carbon reduction and pollution control to strengthen the momentum for green development[3]. Solid waste valorization provides an important pathway for achieving synergy between pollution and carbon reduction.

The rapid expansion of the electric vehicle (EV) industry has driven substantial demand for lithium-ion batteries (LIBs), which dominate EV power storage owing to their high energy density and long cycle life[4-6]. According to the International Energy Agency statistics, global EV sales in 2025 increased by approximately 20% year-over-year, surpassing 20 million units for the first time, with EVs accounting for 25% of all new vehicle sales[7]. China is a major producer and consumer of LIBs, with a production capacity of 735.50 GWh, accounting for more than 70% of the global total[8]. With early-generation EV batteries retiring, China's spent power batteries are projected to exceed 2.6 million metric tons by 2028[9]. Improper treatment of end-of-life (EOL) LIBs may pose safety and environmental risks due to heavy metals, toxic electrolytes, and fluorinated compounds[10]. EOL lithium nickel cobalt manganese oxide (NCM) batteries are particularly valuable for recycling because their cathodes contain lithium (Li), nickel (Ni), and cobalt (Co)[11,12]. Because NCM battery recycling routes differ markedly in energy use, material recovery, and secondary pollution control, evaluating their synergistic reductions in pollution and carbon emissions is essential for optimizing technology selection and advancing a green, low-carbon battery recycling industry[13,14].

Numerous studies have evaluated the environmental benefits of LIB recycling processes. By reducing the demand for primary resource extraction and virgin material production, recycling EOL LIBs can lower environmental burdens and resource consumption[15]. Commercial LIB recycling is currently dominated by pyrometallurgical and hydrometallurgical processes, which primarily focus on recovering high-value metals, whereas closed-loop material regeneration and whole-process environmental optimization remain limited[16]. Compared with conventional pyrometallurgical and hydrometallurgical routes, direct recycling has been reported to offer greater potential to reduce greenhouse gas emissions and water consumption, with reductions of 29.27%−38.15% and 30.07%−41.19%, respectively[17,18], and may further lower carbon dioxide (CO_2) emissions during electrode material regeneration[19,20]. However, other studies have shown that hydrometallurgical treatment may yield greater environmental benefits under specific system boundaries and substitution assumptions, particularly when lithium is recovered as lithium hydroxide (LiOH)[21]. Pyro-hydrometallurgical recycling also offers advantages for improving material recovery performance and resource recovery completeness[22]. These inconsistent findings indicate that the environmental benefits of different recycling processes are influenced by multiple factors, such as battery chemistry and environmental impact categories[23]. Therefore, assessments based on a single environmental indicator are insufficient to fully capture the pollution-reduction effects of recycling processes and their relationship to carbon mitigation.

Because air pollutants and carbon emissions often share common sources, studies on the synergy between pollution and carbon reduction have largely focused on air pollution, where coordination or synergy indices are commonly constructed between pollutants such as particulate matter (PM 2.5) and CO_2 emissions[24-26]. In the field of solid waste valorization, researchers have begun developing life-cycle-based approaches to evaluate the synergistic benefits of pollution and carbon reduction. Some studies have developed synergy coordinate systems, emission-reduction indicator systems, and synergistic evaluation models for

resource recovery technologies, copper slag recycling, and municipal solid waste management[27-29]. The Tapio decoupling model has also been applied to assess the synergistic benefits of pollution and carbon reduction in recycled LIBs. Nevertheless, existing LIB-related studies have mainly compared virgin and recycled batteries or focused on a single hydrometallurgical process, while systematic comparisons across multiple recycling routes remain limited[30]. Therefore, the assessment of synergies between pollution and carbon reduction in EOL LIB recycling remains insufficient. In particular, it remains unclear how different recycling processes perform across multiple pollution-related impact categories and carbon emissions, and which key stages drive their synergistic benefits and optimization potential.

Based on the above considerations, this study applies life cycle assessment (LCA), contribution hotspot analysis, sensitivity analysis, scenario analysis, and a synergy index (SI) for pollution and carbon reduction to evaluate different recycling processes for EOL NCM batteries in China. Using the treatment of 1 kg of EOL NCM batteries as the functional unit, four recycling routes, namely pyrometallurgical, hydrometallurgical, pyro-hydrometallurgical, and direct recycling, are compared across multiple environmental impact categories to identify environmentally preferable pathways. Contribution hotspot and sensitivity analyses are then used to identify the key stages and parameters that drive environmental burdens and synergistic effects. Scenario analysis further evaluates the potential for improvement in technology upgrading, energy-structure transition, and their combined optimization. Finally, the synergistic relationships and potential trade-offs between pollution and carbon reduction are quantified under different scenarios. The research framework of this study is shown in the **Figure. 1.**

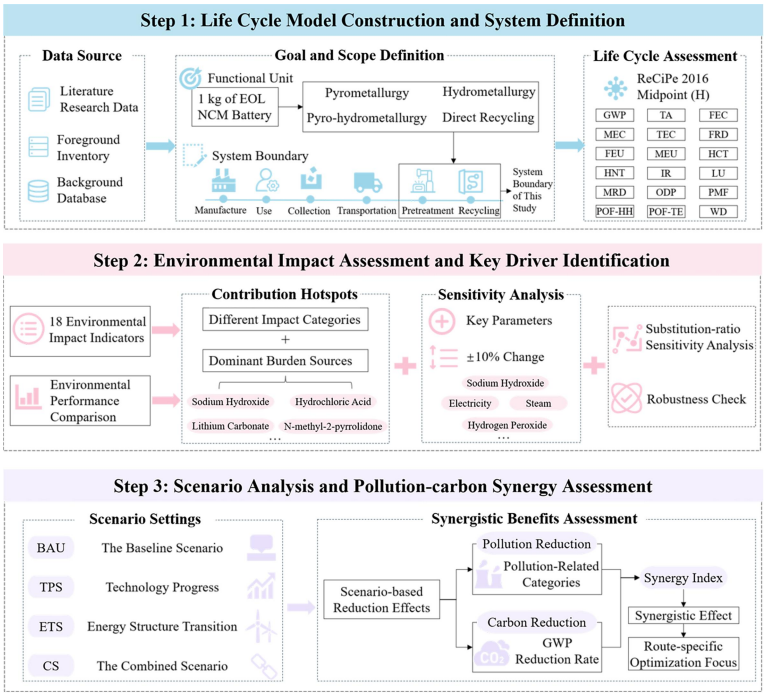

Figure. 1 Research framework. **NOTE:** EOL: end-of-life; NCM: nickel cobalt manganese oxide; GWP: global warming potential; TA: terrestrial acidification; FEC: freshwater ecotoxicity; MEC: marine ecotoxicity; TEC: terrestrial ecotoxicity; FRD: fossil resource depletion; FEU: freshwater eutrophication; MEU: marine eutrophication; HCT: human carcinogenic toxicity; HNT: human noncarcinogenic toxicity; IR: ionizing radiation; LU: land use; MRD: mineral resource depletion; ODP: ozone depletion; PMF: particulate matter formation; POF-HH: photochemical oxidant formation (human health); POF-TE: photochemical oxidant formation (terrestrial ecosystems); WD: water depletion; BAU: the baseline scenario; TPS: technology progress scenario; ETS: energy structure transition scenario; CS: combined scenario. Copyright: The figure was created by the authors using Microsoft PowerPoint software (version 2024; Microsoft Corporation, Redmond, Washington, United States).

2. Methods and Data

2.1 Life Cycle Assessment

2.1.1 Goal and Scope Definition

The functional unit in this study is defined as 1 kg of EOL NCM batteries. The primary function of the assessed systems is to treat an equivalent quantity of battery waste, thereby providing a consistent basis for comparing process-related environmental burdens across the four recycling routes. The system boundary covers the recycling process for EOL NCM batteries, from pretreatment to final material recovery, as well as associated pollutant emissions. Recovered metals, intermediate compounds, and regenerated cathode materials are treated as outputs of the recycling systems. Battery production, collection, use, transportation, and second-life operation processes are excluded from the system boundary[31]. In addition, infrastructure and mechanical equipment are not considered in this study because their contributions to overall environmental impacts are relatively small and relevant data are limited[32]. Four representative NCM battery recycling processes in China are selected for comparative analysis of their synergistic benefits in pollution and carbon reduction. The four recycling routes considered in this study differ in their technological maturity and level of industrial application. Pyrometallurgical, hydrometallurgical, and pyro-hydrometallurgical recycling are relatively established pathways that have been implemented at industrial or commercial scales. In contrast, direct recycling remains an emerging technology and is currently investigated mainly at the laboratory or pilot scale. Therefore, the four routes are regarded as representative technological pathways rather than equally mature industrial practices. Direct recycling is included as a prospective pathway to evaluate its potential

environmental benefits and possible burden-shifting effects relative to the established recycling routes. The process routes and system boundaries of each recycling technology are shown in the **Figure. 2**.

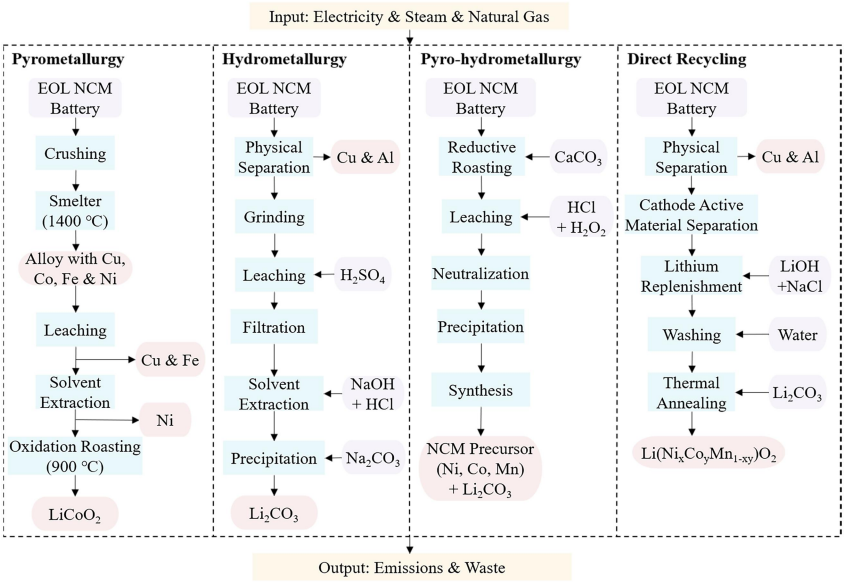

Figure. 2 System boundaries and flowchart of the four processes. **NOTE:** HCl: hydrochloric acid; NaOH: sodium hydroxide; NaCl: sodium chloride; LiOH: lithium hydroxide. Copyright: The figure was created by the authors using Microsoft PowerPoint software (version 2024; Microsoft Corporation, Redmond, Washington, United States).

(a) The pyrometallurgical recycling process is based on high-temperature smelting. After being discharged and dismantled, the battery cells from EOL NCM batteries are fed into a smelting furnace at approximately 1,400 ℃. Organic components, electrolytes, and carbonaceous materials are decomposed or combusted during smelting, while Ni, Co, copper (Cu), and iron (Fe) are enriched in the alloy phase, and Li, aluminum (Al), and manganese (Mn) mainly enter the slag phase. The alloy products are then subjected to inorganic acid leaching, followed by solvent extraction and purification to recover target metals. The recovered metal intermediates can be further processed by oxidation and roasting at approximately 900 ℃ to produce cathode material precursors or regenerated cathode materials[33].

(b) The hydrometallurgical recycling process is based on acid leaching and solution-based separation. EOL NCM batteries are first discharged, dismantled, and mechanically crushed. After physical separation, Cu, Al, and electrode active materials are recovered from the crushed battery mixture. The separated electrode active materials are then ground and leached with sulfuric acid (H_2SO_4) to dissolve Ni, Co, Mn, and Li into the leachate. The dissolved metal ions are selectively separated through pH adjustment and solvent extraction, followed by washing, drying, and crystallization to obtain cobalt sulfate ($CoSO_4$), manganese sulfate ($MnSO_4$), and nickel sulfate ($NiSO_4$). Finally, sodium carbonate (Na_2CO_3) is added to the remaining lithium-containing solution to precipitate and recover Li in the form of lithium carbonate (Li_2CO_3) crystals[34].

(c) The pyro-hydrometallurgical recycling process integrates high-temperature reductive roasting with hydrometallurgical leaching and separation. After pretreatment, EOL NCM batteries enter the reductive roasting stage, in which petroleum coke serves as both a reducing agent and a fuel. During roasting, organic components decompose, and part of the carbonaceous material and carbonate species are converted, generating CO_2 emissions. Meanwhile, valuable metals such as Ni, Co, Mn, and Li are transformed into forms more suitable for subsequent leaching. The roasted products are then leached with hydrochloric acid (HCl), while hydrogen peroxide (H_2O_2) is added to regulate the redox environment and promote metal dissolution. After neutralization, impurity removal, and purification, the target products are recovered via precipitation, crystallization, or precursor synthesis, ultimately yielding NCM precursors and Li_2CO_3[8].

(d) The direct recycling process aims to regenerate cathode active materials from EOL NCM batteries without fully decomposing them into metal salts or precursors. After safe discharging and dismantling, the batteries are mechanically crushed, sieved, and physically separated to recover powders enriched with NCM cathode active materials, along with Cu and Al. The recovered cathode materials are then re-lithiated with LiOH and Li_2CO_3, followed by heating, steam-assisted treatment, or thermal treatment to repair the crystal structure and restore electrochemical performance. The final product is regenerated NCM cathode material[35].

2.1.2 Life Cycle Inventory

Life cycle inventory analysis is the second phase of LCA and aims to quantify the inputs and outputs associated with the life cycle of a product or service[36]. The completeness and accuracy of inventory data directly affect the reliability and applicability of the final results. Following the ISO 14040 standard, the life cycle inventory in this study includes detailed material and energy flows associated with EOL NCM battery recycling[37]. The foreground data were mainly obtained from the literature[8,33-35] and the China lithium-ion battery unit process database[38]. The background data were derived from the Ecoinvent 3.11 database and the high-quality China-specific LCA database, covering processes such as resource extraction, chemical material production, energy production, and the production of related products or by-products. The life cycle models were developed using openLCA software (version 2.6.1; GreenDelta GmbH, Berlin, Germany). Detailed inventory data for the four recycling processes are provided in **Table S1−S4**. The

inventories for pyrometallurgical, hydrometallurgical, and pyro-hydrometallurgical recycling mainly represent established or industrially relevant process conditions, whereas the inventory for direct recycling primarily reflects laboratory- or pilot-scale process data.

2.1.3 Impact Assessment

Life cycle impact assessment evaluates the potential environmental impacts associated with the life cycle of a product or service[39]. In this study, the ReCiPe 2016 Midpoint (H) life cycle impact assessment method is applied to quantify 18 environmental impact categories. These categories include global warming potential (GWP), terrestrial acidification (TA), freshwater ecotoxicity (FEC), marine ecotoxicity (MEC), terrestrial ecotoxicity (TEC), fossil resource depletion (FRD), freshwater eutrophication (FEU), marine eutrophication (MEU), human carcinogenic toxicity (HCT), human noncarcinogenic toxicity (HNT), ionizing radiation (IR), land use (LU), mineral resource depletion (MRD), ozone depletion (ODP), particulate matter formation (PMF), photochemical oxidant formation: human health (POF-HH), photochemical oxidant formation: terrestrial ecosystems (POF-TE), and water depletion (WD). To examine the robustness of the comparison to uncertainty in the displacement of virgin products by recovered materials, an additional substitution-ratio sensitivity analysis is conducted using substitution ratios of 50%, 80%, and 100%. Detailed assumptions, calculations, and results are provided in **Text S1**, **Table S5**, and **Figure S1**.

2.2 Scenario Settings

To further identify the optimization potential for synergistic pollution and carbon reduction across different recycling processes, this study establishes three optimization scenarios based on the baseline scenario (BAU): the technology progress scenario (TPS), the energy structure transition scenario (ETS), and the combined scenario (CS). The scenario design mainly draws on previous studies on emission-reduction pathways in the LIB industrial chain, particularly those concerning technological improvements, the energy transition, and combined mitigation strategies[8,40]. Key parameters are adjusted based on the results of the contribution hotspot and sensitivity analyses. The detailed settings of key parameters for the four scenarios are presented in **Table S6**.

The BAU scenario represents the current operating conditions of the four recycling processes based on the baseline life cycle inventories (**Table S1−S4**). No additional modifications to process parameters, material inputs, energy consumption, or electricity structure are introduced. Therefore, BAU serves as the reference scenario for evaluating the environmental improvement potential of different optimization pathways.

The TPS is developed following the technological optimization approach proposed by Chen *et al*.[40] which evaluates the potential environmental benefits of recycling process improvements by reducing key material and energy inputs. In this study, the specific parameters adjusted under TPS are selected based on the contribution hotspot and sensitivity analyses, thereby reflecting the dominant environmental drivers and process-specific improvement priorities identified for each recycling route. This scenario represents technological improvements that may be achievable in the short- to medium-term under existing process conditions.

The ETS is established based on the energy structure optimization approach proposed by Tian *et al*.[8] Under this scenario, the conventional background electricity mix in the BAU scenario is replaced by a low-carbon electricity mix consistent with the 1.5 °C climate target, while foreground electricity consumption, material inputs, and other process parameters remain unchanged. This setting isolates the environmental effects of electricity decarbonization while maintaining the existing conditions of the recycling process.

The CS is developed with reference to the integrated optimization framework by Tian *et al*.[8] Specifically, reductions in key material or energy inputs are combined with the adoption of the low-carbon electricity mix under the 1.5 ℃ climate target. This scenario is used to evaluate the maximum potential for environmental improvement under the combined effects of process optimization and electricity decarbonization.

By comparing the multi-category environmental impacts of the four recycling processes under BAU, TPS, ETS, and CS, this study further calculates the reduction rates and SI for pollution and carbon, relative to BAU. These indicators are used to assess the synergistic benefits of pollution and carbon reduction under different optimization pathways.

2.3 Synergistic Reduction Benefits Evaluation

To quantify the synergistic effects between pollution and carbon reduction of EOL NCM battery recycling under different optimization scenarios, this study uses the BAU as the reference and follows the approach proposed by Guo *et al*.[28] to calculate the carbon reduction rate, pollution reduction rate, and SI. Let $GWP_{j,0}$ denote the GWP of recycling process j under the BAU, and $GWP_{j,s}$ denote the GWP of recycling process j under scenario s. The carbon reduction rate of process j under scenario s is calculated as follows:

$$CR_{j,s} = \frac{GWP_{j,0} - GWP_{j,s}}{GWP_{j,0}} \quad (1)$$

where $CR_{j,s}$ represents the carbon reduction rate of recycling process j under scenario s. A larger value indicates a greater reduction in GWP relative to the BAU.

In this study, “pollution reduction” refers to life cycle impact categories that are directly related to pollutant emissions and their associated environmental effects, excluding GWP. These categories include TA, FEC, MEC, TEC, FEU, MEU, HCT, HNT, PMF, POF-HH, ODP, and POF-TE. Resource consumption-related indicators, such as FRD, IR, LU, MRD, and WD, do not directly represent pollution reduction and are therefore excluded from the calculation of the pollution reduction rate and the SI. Although the main SI analysis focuses on pollution-related impact categories, the SI values between GWP reduction and all other non-GWP impact categories were also calculated to provide a more complete picture of potential environmental burden shifting. These extended SI results, covering 17 environmental impact categories except GWP, are provided in **Table S7**.

For pollution-related environmental impact category k, let $EI_{j,k,0}$ denotes the impact result of recycling process j under the BAU, and $EI_{j,k,s}$ denotes the corresponding impact result under scenario s. The reduction rate of this impact category is calculated as follows:

$$ER_{j,k,s} = \frac{EI_{j,k,0} - EI_{j,k,s}}{EI_{j,k,0}} \quad (2)$$

where $ER_{j,k,s}$ represents the reduction rate of impact category k for recycling process j under scenario s. When $ER_{j,k,s} > 0$, the impact category is reduced relative to the BAU, indicating an

environmental improvement. When $ER_{j,k,s} < 0$, the impact category increases relative to the BAU, indicating an adverse change or a shift in environmental burden.

To account for differences in the information carried by individual pollution-related impact categories, the entropy weight method is used to determine objective weights for the 12 pollution-related categories based on their BAU environmental impact results across the four recycling routes[41,42]. The derived weights were held constant across the three optimization scenarios to ensure comparability. Accordingly, the entropy-weighted average pollution-related reduction rate (AER) is calculated as:

$$AER_{j,s} = \sum_{k=1}^{12} w_k ER_{j,k,s} \quad (3)$$

where w_k is the entropy-derived weight of pollution-related impact category k, with $\sum_{k=1}^{12} w_k = 1$. The detailed weighting procedure and indicator weights are provided in Supplementary **Text S2** and **Table S8−S9**.

This study further calculates the SI between each pollution-related impact category and carbon reduction:

$$SI_{j,k,s} = \frac{ER_{j,k,s}}{CR_{j,s}} \quad (4)$$

where $SI_{j,k,s}$ represents the degree of synergy between the reduction in pollution-related impact category k and carbon reduction for recycling process j under scenario s. The closer $SI_{j,k,s}$ is to 1, the higher the coordination between pollution and carbon reduction. When $SI_{j,k,s} > 1$, the reduction in the pollution-related impact category is greater than the carbon reduction. When $0 < SI_{j,k,s} < 1$, carbon reduction is more pronounced than pollution reduction. When $SI_{j,k,s} < 0$, carbon emissions and the corresponding pollution-related impact category are not reduced synergistically.

It should be noted that the SI reflects the relative coordination between pollution reduction and carbon reduction, rather than the absolute magnitude of environmental improvement. Therefore, this study jointly considers the carbon reduction rate, pollution reduction rate, and SI to comprehensively evaluate the environmental improvement effects under different scenarios.

3. Results and Discussion

3.1 Environmental Impact of Four Recycling Processes under the Baseline Scenario

3.1.1 Environmental Impact Comparison

Under the BAU and the defined system boundary, the four EOL NCM battery recycling processes show different environmental performance, with direct recycling showing the lowest burdens in most impact categories. As shown in **Table 1**, among the 18 environmental impact indicators, direct recycling exhibits the lowest environmental burdens in 12 categories, including GWP and TA, whereas pyro-hydrometallurgical recycling performs best in the remaining six categories, including FEC and MEC. In contrast, pyrometallurgical recycling exhibits relatively high environmental burdens across 11 categories, while hydrometallurgical recycling exhibits relatively high burdens across 7 categories.

Table 1. Environmental impacts of four recycling technologies for EOL NCM batteries

Impact Category	Unit	Pyrometallurgy Processes	Hydrometallurgical Processes	Pyro-Hydrometallurgy Processes	Direct Recycling Processes
GWP	kg CO_2-eq	7.3080×10^{0}	9.6761×10^{0}	1.9142×10^{0}	1.3462×10^{0}
TA	kg SO_2-eq	6.8957×10^{-2}	5.3430×10^{-2}	6.3667×10^{-3}	5.8751×10^{-3}
FEC	kg 1,4-DCB-eq	5.3619×10^{-1}	4.4965×10^{-1}	5.4872×10^{-2}	6.5008×10^{-2}
MEC	kg 1,4-DCB-eq	6.9819×10^{-1}	5.8375×10^{-1}	7.3654×10^{-2}	8.5990×10^{-2}
TEC	kg 1,4-DCB-eq	2.3331×10^{1}	1.5907×10^{1}	1.8861×10^{0}	4.0188×10^{0}
FRD	kg oil-eq	1.9531×10^{0}	2.8645×10^{0}	5.8344×10^{-1}	3.3205×10^{-1}
FEU	kg P-eq	3.1803×10^{-3}	2.6694×10^{-3}	4.2854×10^{-4}	4.6926×10^{-4}
MEU	kg N-eq	1.9130×10^{-3}	3.6256×10^{-4}	4.2839×10^{-5}	4.8458×10^{-4}
HCT	kg 1,4-DCB-eq	1.5560×10^{0}	1.5172×10^{0}	3.1517×10^{-1}	2.1435×10^{-1}
HNT	kg 1,4-DCB-eq	1.2543×10^{1}	1.0603×10^{1}	2.0467×10^{0}	1.8392×10^{0}
IR	kBq Co-60-eq	4.4389×10^{-1}	4.9000×10^{-1}	3.7129×10^{-2}	2.6325×10^{-2}
LU	m^2a crop-eq	1.4908×10^{-1}	1.6300×10^{-1}	4.2924×10^{-2}	2.4967×10^{-2}
MRD	kg Cu-eq	8.1344×10^{0}	5.4167×10^{-1}	3.9462×10^{-2}	2.0747×10^{0}
ODP	kg CFC-11-eq	2.6408×10^{-6}	1.9524×10^{-6}	4.0346×10^{-7}	2.8826×10^{-7}
PMF	kg $PM_{2.5}$-eq	2.5748×10^{-2}	1.8919×10^{-2}	3.0598×10^{-3}	2.3975×10^{-3}
POF-HH	kg NO_x-eq	2.1101×10^{-2}	2.1433×10^{-2}	5.4822×10^{-3}	3.8864×10^{-3}
POF-TE	kg NO_x-eq	2.1732×10^{-2}	2.2447×10^{-2}	5.6129×10^{-3}	3.9856×10^{-3}
WD	m^3	1.5834×10^{-1}	2.1374×10^{-1}	1.0316×10^{-2}	8.5307×10^{-3}

NOTE: GWP: global warming potential; TA: terrestrial acidification; FEC: freshwater ecotoxicity; MEC: marine ecotoxicity; TEC: terrestrial ecotoxicity; FRD: fossil resource depletion; FEU: freshwater eutrophication; MEU: marine eutrophication; HCT: human carcinogenic toxicity; HNT: human noncarcinogenic toxicity; IR: ionizing radiation; LU: land use; MRD: mineral resource depletion; ODP: ozone depletion; PMF: particulate matter formation; POF-HH: photochemical oxidant formation (human health); POF-TE: photochemical oxidant formation (terrestrial ecosystems); WD: water depletion.

To clarify the composition and sources of environmental impacts, this study further analyzes the contribution of hotspots across different impact categories (**Figure. 3**). Direct recycling exhibits the lowest GWP, at 1.35 kg CO_2-eq, followed by pyro-hydrometallurgical recycling at 1.91 kg CO_2-eq. In contrast, pyrometallurgical and hydrometallurgical recycling show substantially higher GWP values, reaching 7.31 kg CO_2-eq and 9.68 kg CO_2-eq, respectively. The GWP of direct recycling is approximately 81.60%, 86.10%, and 29.70% lower than those of pyrometallurgical, hydrometallurgical, and pyro-hydrometallurgical recycling, respectively. In pyrometallurgical recycling, sodium hydroxide (NaOH) and lithium carbonate (Li_2CO_3) contribute 56.30% and 28.10% of the GWP, respectively, indicating that chemical production and supplementary material inputs are the main sources of carbon emissions. In hydrometallurgical recycling, N-methyl-2-pyrrolidone (NMP) solvent is the largest contributor, accounting for 53.60% of the GWP, followed by electricity consumption at 27.10%. For pyro-hydrometallurgical recycling, electricity consumption dominates the GWP contribution, accounting for 68.80%, followed by HCl at 21.30%.

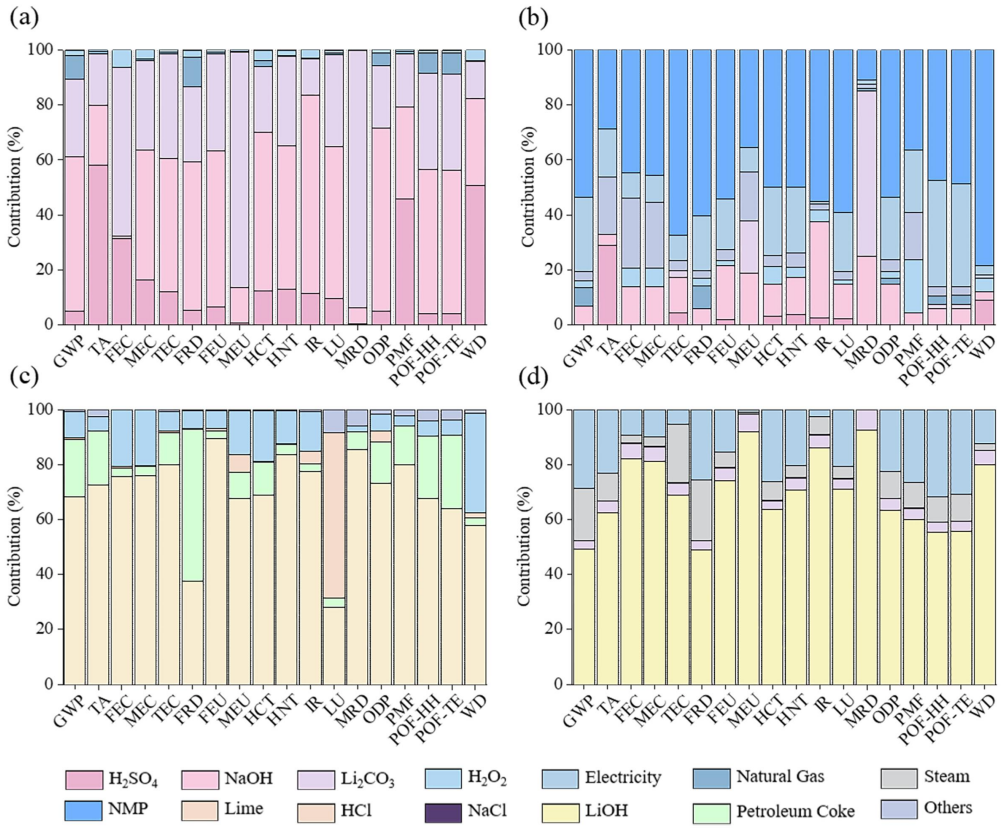

Figure. 3 Key environmental impact contributors of four recycling technologies for EOL NCM batteries. (a) Pyrometallurgy processes; (b) Hydrometallurgical processes; (c) Pyro-hydrometallurgy processes; (d) Direct recycling processes. **NOTE:** H_2SO_4: sulfuric acid; Li_2CO_3: lithium carbonate; H_2O_2: hydrogen peroxide; NMP: N-methyl-2-pyrrolidone. Copyright: The figure was created by the authors using Origin software (version 2022; OriginLab Corporation, Northampton, Massachusetts, United States).

The most pronounced difference among all environmental impact categories occurs in MRD. Pyro-hydrometallurgical recycling shows the lowest impact in this category, at 0.04 kg Cu-eq, whereas pyrometallurgical recycling reaches 8.13 kg Cu-eq, resulting in a maximum-to-minimum ratio of 206.13. The MRD impact of direct recycling is substantially higher than that of pyro-hydrometallurgical recycling, reaching 2.07 kg Cu-eq, approximately 52.57 times the latter. This result suggests that, under the current system boundary and model assumptions, pyro-hydrometallurgical recycling may provide lower net mineral resource burdens, whereas direct recycling relies heavily on lithium-containing chemical inputs. The contribution hotspot results further support this interpretation: LiOH dominates several environmental impact categories in direct recycling, contributing 82.20% of FEC, 74% of FEU, 92.60% of MRD, and 80% of WD. The difference in TEC is also notable, with the impact of direct recycling being 2.13 times that of pyro-hydrometallurgical recycling.

3.1.2 Sensitivity Analysis

To identify the key parameters influencing the environmental impacts of different recycling processes, this study conducts a sensitivity analysis based on the contribution hotspot results. The main material and energy inputs of the four recycling processes are changed by ±10%, and sensitivity coefficients are used to evaluate the response of environmental impact results to parameter changes. A higher sensitivity coefficient indicates a stronger influence of the corresponding parameter on the environmental impact results.

As shown in **Figure. 4**, the sources of environmental sensitivity differ markedly among the recycling processes. For pyrometallurgical recycling, NaOH is the most sensitive parameter overall, with sensitivity coefficients of 0.56 for GWP and 0.72 for IR, whereas electricity shows the lowest average sensitivity coefficient. NMP is the most critical sensitivity parameter for hydrometallurgical recycling. Its average absolute sensitivity coefficient across key

impact categories is 0.45, and its sensitivity coefficient for GWP is 0.54. The highest sensitivity occurs in WD, with a coefficient of 0.79. These results indicate that NMP is not only an important contributor to GWP in hydrometallurgical recycling, but also a key factor affecting WD and several pollution-related impact categories. Changes in the electricity mix also have a noticeable influence on air-pollution-related categories and GWP in hydrometallurgical recycling, with an average absolute sensitivity coefficient of 0.19.

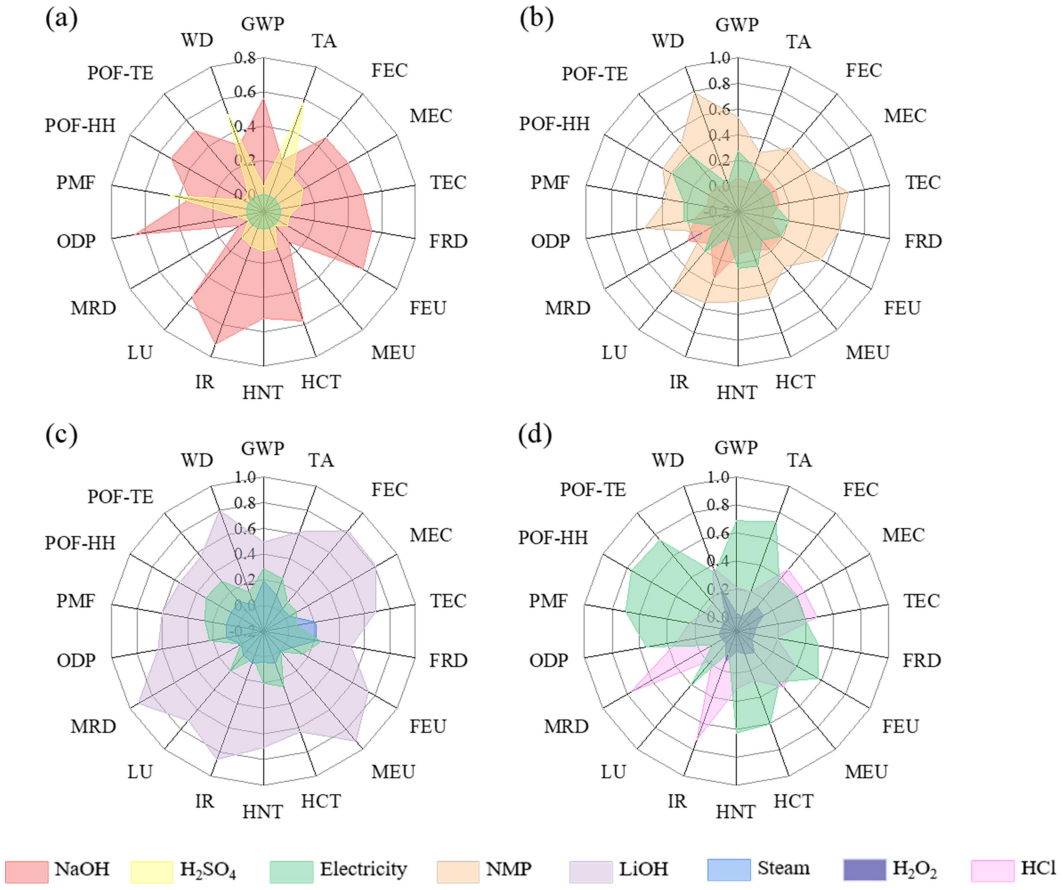

Figure. 4 Sensitivity analysis of the environmental impacts of four processes to changes in major material and energy inputs. (a) Pyrometallurgy processes; (b) Hydrometallurgical processes; (c) Pyro-hydrometallurgy processes; (d) Direct recycling processes. Copyright: Figure was created by the authors using Origin software (version 2022; OriginLab Corporation, Northampton, Massachusetts, United States).

For pyro-hydrometallurgical recycling, electricity is the most sensitive parameter, followed by HCl. H_2O_2 shows a relatively low average sensitivity coefficient of 0.05, but its influence on WD is more pronounced, with a maximum sensitivity coefficient of 0.24. For direct recycling, LiOH is the dominant sensitivity parameter, with an average absolute sensitivity coefficient of 0.68 across key impact categories, the highest among all parameters in the four recycling processes. Its sensitivity coefficient for GWP is 0.49. Combined with the contribution hotspot results under the baseline scenario, these findings indicate that LiOH is the dominant contributor to multiple environmental impacts in direct recycling. Therefore, its input amount, production pathway, and substitution source can substantially affect the overall environmental performance of direct recycling.

Overall, the sensitivity analysis suggests that scenario optimization should be process-specific. Pyrometallurgical recycling should focus on reducing chemical inputs, such as NaOH and H_2SO_4, in subsequent leaching and separation processes; hydrometallurgical recycling should prioritize optimizing the NMP solvent system; pyro-hydrometallurgical recycling should focus on decarbonizing electricity and reducing HCl; and direct recycling should optimize Li replenishment using LiOH.

3.2 Synergistic Benefits of Four Recycling Processes under Optimized Conditions

Using the ReCiPe 2016 midpoint method and the BAU as the reference, this study calculates the reduction rates of 18 environmental impact categories for the four recycling processes under three optimization scenarios. Based on the SI, particular attention is given to the synergistic benefits of pollution and carbon reduction.

As shown in the **Figure. 5**, the GWP reduction rates differ substantially among the recycling processes under the optimization scenarios. For pyrometallurgical recycling, the GWP reduction rates under TPS and CS are 6.14% and 6.31%, respectively, whereas ETS achieves only 0.19%. This indicates that energy structure transition contributes little to carbon reduction in this process. For hydrometallurgical recycling, carbon reduction increases progressively across the scenarios, with GWP reduction rates of 8.75%, 25.36%, and 31.57% under TPS, ETS, and CS, respectively. The pronounced carbon reduction under ETS can be attributed to the substantial influence of cleaner electricity on

electricity-intensive stages in hydrometallurgical recycling. Pyro-hydrometallurgical recycling shows the largest carbon reduction potential, with GWP reduction rates of 64.43% under ETS and 67.30% under CS, compared with 9.31% under TPS, indicating its high sensitivity to changes in the electricity structure. Direct recycling achieves GWP reductions of 9.69%, 26.92%, and 33.92% under TPS, ETS, and CS, respectively, indicating an intermediate overall carbon-reduction potential.

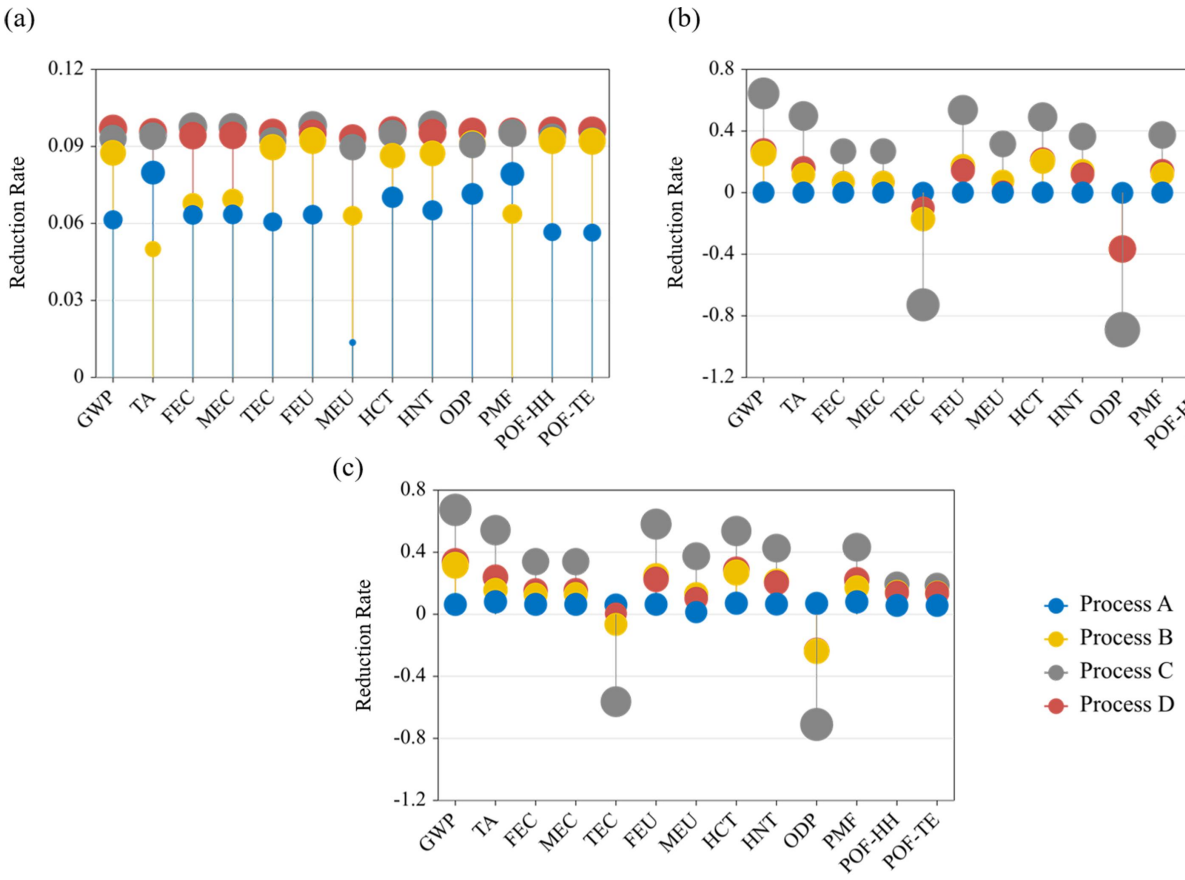

Figure. 5 Comparison of emission reduction performance under three optimization scenarios. (a) The technology progress scenario; (b) The energy structure transition scenario; (c) The combined scenario. Processes A-D represent: A: pyrometallurgy recycling; B: hydrometallurgy recycling; C: pyro-hydrometallurgy recycling; D: direct recycling. Copyright: Figure was created by the authors using Python software (version 3.11; Python Software Foundation, Beaverton, Oregon, United States).

The reduction rates of pollution-related impact categories show more pronounced unevenness across processes and scenarios. Under the TPS, all four recycling processes achieve positive rates of pollution reduction. Direct recycling exhibits the most balanced performance, with reduction rates ranging from 9.30% to 9.60% across impact categories. Pyro-hydrometallurgical and hydrometallurgical recycling follow, with most impact categories ranging from 7.20%–9.80% and 5%–9.20%, respectively, while pyrometallurgical recycling is mainly concentrated around 6%–8%.

Under the ETS, pollution reduction performance becomes highly differentiated. Hydrometallurgical and pyro-hydrometallurgical recycling show substantial improvements in some impact categories. For hydrometallurgical recycling, reductions in TA, PMF, and HCT range from 11.80% to 20.30%. For pyro-hydrometallurgical recycling, reductions in TA and FEC reach up to 49.80%–53.70%. However, both processes show large negative reduction rates for TEC and ODP, with hydrometallurgical recycling rising by 17.20% and 36.60%, and pyro-hydrometallurgical recycling by 72.90% and 89%, respectively. This suggests that although cleaner electricity substitution can substantially reduce GWP, changes in upstream emission profiles may intensify certain non-carbon environmental burdens. By contrast, pyrometallurgical and direct recycling show relatively small fluctuations under the ETS, with pollution reduction rates remaining at low positive levels or showing only slight negative values.

Under the CS, the positive pollution-reduction effects of hydrometallurgical and pyro-hydrometallurgical recycling are further enhanced relative to the ETS, but the negative effects on TEC and ODP remain severe, indicating a pronounced imbalance in pollution reduction. Overall, the dispersion of pollution reduction rates across impact categories is much greater under the ETS and CS than under the TPS. These results suggest that electricity decarbonization alone may lead to substantial carbon reductions but uneven reductions in pollution, especially for electricity-intensive recycling routes.

Based on the above reduction results, the synergistic benefits of pollution and carbon reduction are further analyzed (**Figure. 6**). Pyrometallurgical recycling shows the strongest synergy under the TPS and CS. Under TPS, GWP is reduced by 6.14%, and most pollution-related synergy indicators have SI values greater than 1, including TA (1.3), FEC and MEC (1.03 and 1.03), and PMF

(1.29). This indicates that technological upgrading can provide synergistic control benefits for the environmentally intensive stages of conventional pyrometallurgical recycling. However, under ETS, the GWP reduction of pyrometallurgical recycling is only 0.19%, indicating a limited carbon mitigation effect. Under CS, the GWP reduction increases to 6.31%, and strong synergistic effects re-emerge.

Hydrometallurgical and pyro-hydrometallurgical recycling both achieve their best synergistic performance under the TPS. Under the ETS and CS, although these two processes achieve the largest GWP reductions, namely 25.36%−31.57% for hydrometallurgical recycling and 64.43%−67.30% for pyro-hydrometallurgical recycling, their pollution reductions are smaller than their carbon reductions, indicating weak synergy. In particular, hydrometallurgical recycling shows pronounced negative synergy for TEC and ODP, with SI as low as -1.44 and -1.38, respectively. Under the ETS and CS, most pollution-related SI values for pyro-hydrometallurgical recycling remain substantially below 1, indicating a clear pattern of strong carbon reduction but comparatively weak pollution mitigation.

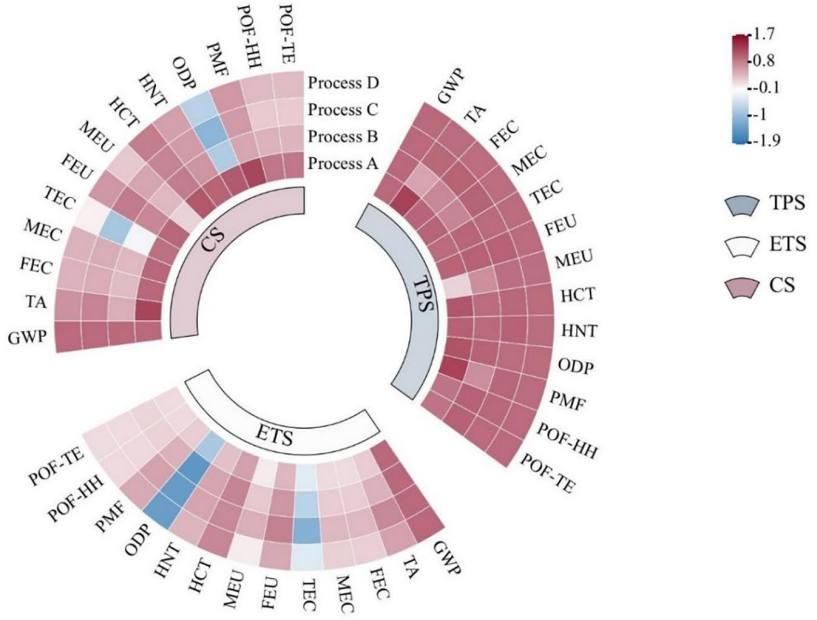

Figure. 6 Synergistic benefits of pollutant emissions reductions and GWP reductions under three scenarios. Processes A-D represent: A: pyrometallurgy recycling; B: hydrometallurgy recycling; C: pyro-hydrometallurgy recycling; D: direct recycling. Copyright: The figure was created by the authors using Python software (version 3.11; Python Software Foundation, Beaverton, Oregon, United States).

Direct recycling shows the most balanced performance under the TPS. Its GWP is reduced by 9.69%, while the entropy-weighted AER reaches 9.54%. Meanwhile, all pollution-related SI values range from 0.96 to 0.99, indicating nearly synchronized reductions in pollution and carbon. Under the ETS and CS, GWP reductions increase to 26.92% and 33.92%, respectively, whereas the weighted AER values are only 5.63% and 14.61%. This indicates that carbon mitigation becomes considerably stronger than pollution reduction under electricity decarbonization and combined optimization, although the overall pollution-related impacts still show positive reductions.

Considering the overall performance of the four recycling processes, the TPS offers the best synergistic benefits. Under this scenario, pyrometallurgical and pyro-hydrometallurgical recycling show strong synergy, direct recycling has SI values close to 1, and hydrometallurgical recycling shows relatively weak but not severely negative synergy. Thus, the synergistic direction of the four processes is highly consistent. By contrast, although the ETS and CS scenarios achieve greater carbon reductions, they also lead to negative synergy in some ecotoxicity-related categories for hydrometallurgical and pyro-hydrometallurgical recycling, resulting in poorer overall consistency in synergy.

3.3 Discussion

This study reveals a complex relationship between environmental performance and synergistic benefits of pollution and carbon reduction in EOL NCM battery recycling. The environmental performance of recycling processes is jointly determined by material transformation pathways, key material inputs, energy structure, and upstream supply chains. Therefore, comparisons across multiple environmental impact categories are necessary to avoid one-sided judgments based on a single indicator[43]. The comparative results do not indicate that any single recycling route is environmentally preferable across all impact categories. Under the BAU and the defined system boundary, direct recycling exhibits the lowest impacts in 12 of the 18 midpoint categories, including GWP, whereas pyro-hydrometallurgical recycling performs best in the remaining six categories. These results indicate technology-specific environmental advantages rather than an unconditional overall ranking of the four recycling routes. Direct recycling shows lower burdens, particularly for GWP and several emission-related categories, whereas pyro-hydrometallurgical recycling exhibits advantages in selected resource- and toxicity-related categories. The hotspot and sensitivity results demonstrate that the dominant environmental constraints are process-specific: chemical inputs dominate pyrometallurgical recycling; solvent and electricity use constrain hydrometallurgical recycling; electricity and acid-leaching agents drive pyro-hydrometallurgical recycling; and lithium replenishment is the key determinant of direct recycling.

The relatively low burdens of direct recycling in GWP and

several emission-related impact categories are mainly attributable to this shorter pathway[35]. Unlike pyrometallurgical and hydrometallurgical routes, which decompose cathode materials into metals or precursors and then resynthesize battery materials, direct recycling repairs or regenerates cathode materials while preserving part of their original structure and embedded energy from material production. The study by Ciez and Whitacre similarly indicates that direct recycling generally has greater GWP mitigation potential because it retains part of the structural value and embedded energy of cathode materials[18]. The results of this study are broadly consistent with this conclusion, but further show that the advantages of direct recycling are not unconditional. Previous studies have shown that the type of lithium source and the production pathway of LiOH can significantly affect the life-cycle environmental footprint of battery materials and products[44]. If lithium replenishment efficiency is low or the lithium source itself has a high environmental burden, direct recycling may create new environmental pressures regarding MRD and selected toxicity-related categories. The substitution-ratio sensitivity analysis further supports the robustness of the GWP-based comparison while indicating greater sensitivity in several non-carbon-impact categories. Direct recycling consistently retains the lowest GWP across the investigated substitution ratios, with GWP decreasing from 1.35 to 0.12, -0.61, and -1.10 at substitution ratios of 50%, 80%, and 100%, respectively. Moreover, the best-performing route remains unchanged for 12 of the 18 midpoint impact categories (66.70%). Previous studies show that the environmental benefits of recycled materials depend on their technical substitutability for virgin products and on the treatment of secondary materials in LCA[45,46]. Therefore, although the low-carbon advantage of direct recycling is relatively robust, comparisons across non-carbon impact categories should still consider recovered-product quality and practical substitution potential.

Pyro-hydrometallurgical recycling shows advantages across several resource- and toxicity-related impact categories, suggesting that process integration can partially offset the limitations of single-route recycling. Pyrometallurgical recycling is characterized by strong feedstock adaptability and high industrial maturity, whereas hydrometallurgical recycling provides effective metal extraction and separation. These characteristics also lead to distinct environmental profiles: pyrometallurgical recycling involves energy-intensive thermal treatment and subsequent refining processes, while hydrometallurgical recycling relies more strongly on chemical reagents, solvents, and electricity. By combining front-end thermal treatment with subsequent hydrometallurgical separation, the integrated route alters the material and energy requirements of subsequent recovery processes, as reflected in its comparatively low burdens across several resource- and toxicity-related impact categories. Therefore, the environmental advantage of pyro-hydrometallurgical recycling does not lie in achieving the lowest GWP, but is reflected in its relatively low impacts in selected resource- and toxicity-related categories. This finding further illustrates that comparisons of recycling routes depend on the environmental dimension considered and should not be reduced to a single GWP-based ranking. Existing reviews have noted that pyrometallurgical, hydrometallurgical, and direct recycling routes each have distinct advantages and limitations, and that process selection often requires trade-offs among recovery efficiency, product quality, energy consumption, and pollution control[6]. The hotspot and sensitivity results further indicate that the environmental performance of pyro-hydrometallurgical recycling is particularly influenced by electricity and acid-leaching inputs, highlighting the importance of these factors in interpreting its overall environmental profile.

Pyrometallurgical and hydrometallurgical recycling remain important and technologically mature routes for EOL LIB treatment, but their environmental impacts arise from distinct process mechanisms[8]. For pyrometallurgical recycling, the burden does not arise solely from high-temperature smelting; downstream acid leaching, separation, and supplementary material inputs also play important roles. Thus, green upgrading of pyrometallurgical recycling should combine energy-saving furnace operation and waste-heat recovery with reduced chemical inputs, slag valorization, and more complete recovery of valuable components. For hydrometallurgical recycling, the main bottleneck lies in solvent and electricity consumption. NMP affects not only GWP, but also WD, FEC, and other pollution-related impact categories, indicating that the environmental cost of the solvent system is a key constraint. Future development of hydrometallurgical routes should therefore prioritize closed-loop solvent circulation, lower-impact solvent substitution, and extraction system optimization, rather than pursuing higher metal leaching rates alone.

The scenario results further demonstrate that large carbon reductions do not necessarily correspond to strong pollution-carbon synergy. Optimization strategies that focus primarily on GWP reduction through electricity decarbonization may overlook non-carbon burdens associated with chemicals, solvents, metals, and upstream production processes[47]. Energy structure transition can markedly reduce the GWP of electricity-dependent processes, but its effects on pollution-related impact categories are unstable and may even increase some non-carbon environmental burdens. This is because low-carbon electricity substitution primarily affects the carbon dimension, whereas a combination of chemicals, solvents, metals, and upstream production processes shapes pollution-related impacts. Changes in the energy system may therefore alter upstream emission profiles and resource input structures, resulting in environmental burden shifting, where GWP decreases while certain impact categories increase. This trade-off is particularly evident for pyro-hydrometallurgical recycling: although ETS reduces its GWP by 64.43%, the associated TEC and ODP impacts increase by 72.90% and 89%, respectively.

By contrast, the TPS shows more stable synergistic benefits because it directly targets the sources of environmental burdens. Rather than merely changing emission factors, technological progress reduces the material and energy inputs that give rise to multiple environmental burdens. As a result, pollution reduction and carbon mitigation are more likely to proceed synchronously. Direct recycling provides a representative example: under TPS, its GWP decreases by 9.69%, while the SI values across all pollution-related categories remain within a narrow range of 0.96 to 0.99, indicating nearly synchronized reductions in pollution and carbon. From a synergy perspective, source-oriented process optimization is therefore more robust than energy substitution alone. Although the CS has greater absolute reduction potential, it does not necessarily produce a higher SI. Combined optimization should therefore not be understood as a simple superposition of technological progress and energy decarbonization. Instead, it

should examine whether different measures generate consistent environmental effects across carbon and pollution-related categories. For enterprises and policymakers, recycling process evaluation should move beyond single indicators such as GWP or metal recovery rates toward an integrated framework that considers carbon mitigation, pollution reduction, resource consumption, and potential environmental burden shifting. This is consistent with previous calls for more systematic, design-friendly, and closed-loop management of battery recycling systems[30,47].

4. Conclusions

This study develops an integrated assessment framework that combines multi-category life cycle assessment, contribution hotspot analysis, sensitivity analysis, scenario analysis, and a pollution-carbon SI to evaluate four representative recycling routes for EOL NCM batteries. The results demonstrate that recycling route selection cannot be based on a single environmental indicator. Although direct recycling exhibits comparatively favorable overall environmental performance under BAU, its advantages are accompanied by potential burden shifting in selected resource- and toxicity-related impact categories. The scenario results further indicate that technological progress generally produces more stable pollution-carbon synergies than electricity decarbonization alone, whereas the combined implementation of process optimization and a low-carbon electricity mix offers the greatest overall potential for environmental improvement.

The findings provide process-specific implications for industrial optimization. Direct recycling should prioritize improving lithium-replenishment efficiency and reducing the consumption of lithium-containing reagents, although its prospective environmental advantages require further validation at the industrial scale. Hydrometallurgical recycling should strengthen solvent recovery, reduce solvent and reagent consumption, and increase the use of low-carbon electricity. Pyro-hydrometallurgical recycling can benefit substantially from decarbonization of electricity, improved process energy efficiency, and reduced acid consumption, whereas pyrometallurgical recycling requires greater attention to key chemical inputs and downstream refining processes. More broadly, the selection and optimization of recycling technologies should simultaneously consider carbon mitigation, pollution reduction, resource consumption, and potential environmental burden shifting rather than rely exclusively on global warming potential or metal recovery efficiency.

This study has several limitations. The foreground inventories are mainly literature-derived and may change with geography, technology, temporal coverage, and technological maturity; direct recycling data largely reflect laboratory or pilot conditions and should therefore be interpreted prospectively. The assessment does not explicitly distinguish NCM grades, degradation states, or mixed feedstocks, and the input-based functional unit does not capture impacts per unit of recovered metal or regenerated cathode material. Scale-up effects, economic costs, and systematic uncertainty propagation are also outside the current scope. Future studies should incorporate chemistry- and degradation-state-specific inventories, industrial-scale data, output-based recovery metrics, and techno-economic and uncertainty analyses to verify the robustness and industrial feasibility of the identified pathways.

Author Contributions

Xi Tian: conceptualization, methodology, validation, writing-review and editing, supervision, project administration, funding acquisition. Ziying Zhang: methodology, validation, formal analysis, writing-original draft preparation, data curation, visualization. Wei Liu: conceptualization, validation, formal analysis, writing-review and editing, data curation, visualization. Xinxue Lai: software, investigation, data curation. Tongzhu Zhang: software, investigation, data curation. Hu Liu: investigation, resources, data curation. Yaobin Liu: conceptualization, investigation, resources. All authors have read and agreed to the published version of the manuscript.

Data Availability

Data will be made available on request.

Conflicts of Interest

The authors declare no competing financial interests.

Funding

This study was supported by the National Natural Science Foundation of China (Grant No. 52270181), Jiangxi Province Key R&D Plan Projects (Grant No. 20232BBG70005), and Jiangxi Provincial Natural Science Foundation for Distinguished Young Scholars (Grant No. 20242BAB23050).

Supplementary Materials

Please refer to the **attachment** for details.

References

[1] Ma R, Tao S, Sun X, *et al.* Pathway decisions for reuse and recycling of retired lithium-ion batteries considering economic and environmental functions [J]. *Nature Communications*. 2024, 15: 1-14. [Google Scholar] [CrossRef]

[2] Zhang L, Ruan J, Zhang Z, *et al.* City-level pathways to carbon peak and neutrality in China [J]. *Cell Reports Sustainability*. 2024, 1 (5): 1-15. [Google Scholar] [CrossRef]

[3] Sun B, Bian C, Dou C. Comprehensive green transformation of economic and social development during the 15th Five-Year Plan period: Key tasks and reform measures [J]. *Ecological Economy*. 2026, 42 (6): 10-22. (In Chinese).

[4] Sanguesa JA, Torres-Sanz V, Garrido P, *et al.* A Review on Electric Vehicles: Technologies and Challenges [J]. *Smart Cities*. 2021, 4: 372-404. [Google Scholar] [CrossRef]

[5] Harvey LDD. Rethinking electric vehicle subsidies, rediscovering energy efficiency [J]. *Energy Policy*. 2020, 146: 1-13. [Google Scholar] [CrossRef]

[6] Lai X, Chen Q, Tang X, *et al.* Critical review of life cycle assessment of lithium-ion batteries for electric vehicles: A lifespan perspective [J]. *eTransportation*. 2022, 12: 1-22. [Google Scholar] [CrossRef]

[7] International Energy Agency. *Global EV Outlook 2026: Growing sales amid an energy crisis* [R]. 2026: 1-288. Available online: https://www.iea.org/reports/global-ev-outlook-2026 (accessed on 20 August 2026).

[8] Tian X, Peng F, McKechnie J, *et al*. Sustainable battery recycling through spatial and technological alignment [J]. *Nature Sustainability*. 2026. [Google Scholar] [CrossRef]
[9] Zhou Y, Cui XD, Lin AJ, *et al*. Environmental life cycle assessment on the recycling processes of power batteries for new energy vehicles [J]. *Journal of Cleaner Production*. 2025, 488: 1-11. [Google Scholar] [CrossRef]
[10] He T, Zhao J, Chen D, *et al*. Self-actuated leaching and integrated separation of spent lithium-ion batteries cathode and anode sheets [J]. *Separation and Purification Technology*. 2024, 345: 1-12. [Google Scholar] [CrossRef]
[11] Wang M, Liu K, Dutta S, *et al*. Recycling of lithium iron phosphate batteries: status, technologies, challenges, and prospects [J]. *Renewable and Sustainable Energy Reviews*. 2022, 163: 1-16. [Google Scholar] [CrossRef]
[12] Tian X, Peng F, Chen X, *et al*. Management of spent power batteries in China: Progress, policies, and challenges [J]. *Renewable and Sustainable Energy Reviews*. 2025, 219: 1-17. [Google Scholar] [CrossRef]
[13] Li P, Luo S, Zhang L, *et al*. Progress, challenges, and prospects of spent lithium-ion batteries recycling: a review [J]. *Journal of Energy Chemistry*. 2024, 89, 144-171. [Google Scholar] [CrossRef]
[14] Biswal BK, Zhang B, Thi Minh Tran P, *et al*. Recycling of spent lithium-ion batteries for a sustainable future: recent advancements [J]. *Chemical Society Reviews*. 2024, 53 (11): 5552-5592. [Google Scholar] [CrossRef]
[15] Li L, Zhang X, Li M, *et al*. The recycling of spent lithium-ion batteries: a review of current processes and technologies [J]. *Electrochemical Energy Reviews*. 2018, 1 (4): 461-482. [Google Scholar] [CrossRef]
[16] Sommerville R, Zhu P, Rajaeifar M A, *et al*. A qualitative assessment of lithium ion battery recycling processes [J]. *Resources, Conservation and Recycling*. 2021, 165: 1-11. [Google Scholar] [CrossRef]
[17] Yu M, Bai B, Xiong S, *et al*. Evaluating environmental impacts and economic performance of remanufacturing electric vehicle lithium-ion batteries [J]. *Journal of Cleaner Production*. 2021, 321: 1-11. [Google Scholar] [CrossRef]
[18] Ciez R E, Whitacre J F. Examining different recycling processes for lithium-ion batteries [J]. *Nature Sustainability*. 2019, 2 (2): 148-156. [Google Scholar] [CrossRef]
[19] Wang J, Ma J, Zhuang Z, *et al*. Toward direct regeneration of spent lithium-ion batteries: a next-generation recycling method [J]. *Chemical Reviews*. 2024, 124 (5): 2839-2887. [Google Scholar] [CrossRef]
[20] Xu P, Tan D H S, Jiao B, *et al*. A Materials Perspective on Direct Recycling of Lithium-Ion Batteries: Principles, Challenges and Opportunities [J]. *Advanced Functional Materials*. 2023, 33 (14): 1-20. [Google Scholar] [CrossRef]
[21] Kallitsis E, Korre A, Kelsall G H. Life cycle assessment of recycling options for automotive Li-ion battery packs [J]. *Journal of Cleaner Production*. 2022, 371: 1-13. [Google Scholar] [CrossRef]
[22] Rey I, Vallejo C, Santiago G, *et al*. Environmental impacts of graphite recycling from spent lithium-ion batteries based on life cycle assessment [J]. *ACS Sustainable Chemistry & Engineering*. 2021, 9 (43): 14488-14501. [Google Scholar] [CrossRef]
[23] Liu Z, Sederholm J G, Lan K W, *et al*. Life cycle assessment of hydrometallurgical recycling for cathode active materials [J]. *Journal of Power Sources*. 2023, 580: 1-10. [Google Scholar] [CrossRef]
[24] Li S, Wang S, Wu Q, *et al*. Integrated benefits of synergistically reducing air pollutants and carbon dioxide in China [J]. *Environmental Science & Technology*. 2024, 58 (32), 14193-14202. [Google Scholar] [CrossRef]
[25] Liu K, Ren G, Dong S, *et al*. The synergy between pollution reduction and carbon reduction in Chinese cities and its influencing factors [J]. *Sustainable Cities and Society*. 2024, 106: 1-12. [Google Scholar] [CrossRef]
[26] Xian B, Xu Y, Chen W, *et al*. Co-benefits of policies to reduce air pollution and carbon emissions in China [J]. *Environmental Impact Assessment Review*. 2024, 104: 1-14. [Google Scholar] [CrossRef]
[27] Guo D, Zhang S, Dai Z, *et al*. Synergistic benefits of pollution and carbon reduction in collaborative domestic solid waste disposal: a life cycle perspective [J]. *Environmental Impact Assessment Review*. 2025, 114: 1-9. [Google Scholar] [CrossRef]
[28] Guo D, Zhang S, Hou H, *et al*. Synergistic evaluation methodology for pollution and carbon reduction in the field of solid waste resource utilization [J]. *Environmental Impact Assessment Review*. 2024, 108: 1-9. [Google Scholar] [CrossRef]
[29] Zhang Y, Yang Y, Guo D, *et al*. Synergistic environmental benefits from copper slag recycling in China: pollutant mitigation and carbon reduction [J]. *Journal of Environmental Management*. 2024, 370: 1-9. [Google Scholar] [CrossRef]
[30] Zhang J, Hu G, Mu X. Environmental benefits assessment of closed-loop recycling for power batteries: a focus on cathode material recycling [J]. *Clean Technologies and Environmental Policy*. 2026, 28: 1-13. [Google Scholar] [CrossRef]
[31] Zhu X, Jin Q, Ye Z. Life cycle environmental and economic assessment of alumina recovery from secondary aluminum dross in China [J]. *Journal of Cleaner Production*. 2020, 277: 1-10. [Google Scholar] [CrossRef]
[32] Tian X, Ma Q, Xie J, *et al*. Environmental impact and economic assessment of recycling lithium iron phosphate battery cathodes: Comparison of major processes in China [J]. *Resources, Conservation and Recycling*. 2024, 203: 1-11. [Google Scholar] [CrossRef]
[33] Wang Y, Tang B, Shen M, *et al*. Environmental impact assessment of second life and recycling for $LiFePO_4$ power batteries in China [J]. *Journal of Environmental Management*. 2022, 314: 1-9. [Google Scholar] [CrossRef]
[34] Chen Q, Lai X, Hou Y, *et al*. Investigating the environmental impacts of different direct material recycling and battery remanufacturing technologies on two types of retired lithium-ion batteries from electric vehicles in China [J]. *Separation and Purification Technology*. 2023, 308: 1-14. [Google Scholar] [CrossRef]
[35] Xu P, Yang Z, Yu X, *et al*. Design and optimization of the direct recycling of spent Li-ion battery cathode materials [J]. *ACS Sustainable Chemistry & Engineering*. 2021, 9 (12): 4543-4553. [Google Scholar] [CrossRef]
[36] Liu W, Zhao R, Wu J, *et al*. Comparative analysis of pressure–temperature swing adsorption processes integrated with different energy-recovery configurations for SF_6 recycling [J]. *Applied Thermal Engineering*. 2026, 300: 1-19. [Google Scholar] [CrossRef]
[37] Feng T, Guo W, Li Q, *et al*. Life cycle assessment of lithium nickel cobalt manganese oxide batteries and lithium iron phosphate batteries for electric vehicles in China [J]. *Journal of Energy Storage*. 2022, 52: 1-12. [Google Scholar] [CrossRef]
[38] Tian X, Li H, Peng F, *et al*. China-specific unit process dataset for lithium-ion batteries [J]. *Resources, Conservation and Recycling*.

2024, 211: 1-6. [Google Scholar] [CrossRef]

[39] Van Stijn A, Malabi Eberhardt L C, Wouterszoon Jansen B, *et al*. A Circular Economy Life Cycle Assessment (CE-LCA) model for building components [J]. *Resources, Conservation and Recycling*. 2021, 174: 1-34. [Google Scholar] [CrossRef]

[40] Chen L, Peng F, Bieryt K, *et al*. From mining to recycling: identifying carbon mitigation pathways across the full life cycle of China's lithium-ion battery industry [J]. *Journal of Cleaner Production*. 2025, 518: 1-11. [Google Scholar] [CrossRef]

[41] Zhang H, Xue B, Li S, *et al*. Life cycle environmental impact assessment for battery-powered electric vehicles at the global and regional levels [J]. *Scientific Reports*. 2023, 13: 1-12. [Google Scholar] [CrossRef]

[42] Öztürk M, Evin E, Özkan A, *et al*. Comparison of waste lithium-ion batteries recycling methods by different decision making techniques [J]. *Environmental Research and Technology*. 2023, 6 (3), 226-241. [Google Scholar] [CrossRef]

[43] Harper G. Recycling lithium-ion batteries from electric vehicles [J]. *Nature*. 2019, 575: 75-86. [Google Scholar] [CrossRef]

[44] Kelly J C, Wang M, Dai Q, *et al*. Energy, greenhouse gas, and water life cycle analysis of lithium carbonate and lithium hydroxide monohydrate from brine and ore resources and their use in lithium ion battery cathodes and lithium ion batteries [J]. *Resources, Conservation and Recycling*. 2021, 174: 1-12. [Google Scholar] [CrossRef]

[45] Sanabria Garcia E, Huysveld S, Nhu T T, *et al*. Technical substitutability of recycled materials in life cycle assessment: a comprehensive review and framework for quantification [J]. *Waste Management*. 2023, 171: 324-336. [Google Scholar] [CrossRef]

[46] Husmann J, Blömeke S, Cerdas F, *et al*. Environmental assessment of secondary materials from battery recycling process chains: the influence of recycling processes and modelling choices [J]. *Procedia CIRP*. 2023, 116: 29-34. [Google Scholar] [CrossRef]

[47] Mrozik W, Rajaeifar M A, Heidrich O, *et al*. Environmental impacts, pollution sources and pathways of spent lithium-ion batteries [J]. *Energy & Environmental Science*. 2021, 14 (12): 6099-6121. [Google Scholar] [CrossRef]